Aquatic Toxicology 273 (2024) 107016

Contents lists available at ScienceDirect

Aquatic Toxicology

journal homepage: www.elsevier.com/locate/aqtox

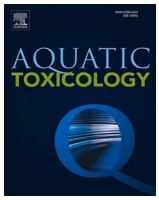

Chronic exposure to environmental concentrations of benzo[a]pyrene causes multifaceted toxic effects of developmental compromise, redox imbalance, and modulated transcriptional profiles in the early life stages of marine medaka (*Oryzias melastigma*)

Rabia Zeb [a], Xiaohan Yin [a], Fangyi Chen [a,b,c], Ke-Jian Wang [a,b,c,*]

[a] State Key Laboratory of Marine Environmental Science, College of Ocean & Earth Sciences, Xiamen University, Xiamen, Fujian, PR China
[b] State-Province Joint Engineering Laboratory of Marine Bioproducts and Technology, College of Ocean & Earth Sciences, Xiamen University, Xiamen, Fujian, PR China
[c] Fujian Innovation Research Institute for Marine Biological Antimicrobial Peptide Industrial Technology, College of Ocean & Earth Sciences, Xiamen University, Xiamen, Fujian, PR China

ARTICLE INFO

Keywords:
Marine medaka
Benzo[a]pyrene
Deformities
Oxidative stress
Apoptosis

ABSTRACT

Polycyclic aromatic hydrocarbons (PAHs) accumulate and integrate into aquatic environments, raising concerns about the well-being and safety of aquatic ecosystems. Benzo[a]pyrene (BaP), a persistent PAH commonly detected in the environment, has been extensively studied. However, the broader multifaceted toxicity potential of BaP on the early life stages of marine fish during chronic exposure to environmentally relevant concentrations needs further exploration. To fill these knowledge gaps, this study assessed the *in vivo* biotoxicity of BaP (1, 4, and 8 μg/L) in marine medaka (*Oryzias melastigma*) during early development over a 30-day exposure period. The investigation included morphological, biochemical, and molecular-level analyses to capture the broader potential of BaP toxicity. Morphological analyses showed that exposure to BaP resulted in skeletal curvatures, heart anomalies, growth retardation, elevated mortality, delayed and reduced hatching rates. Biochemical analyses revealed that BaP exposure not only created oxidative stress but also disrupted the activities of antioxidant enzymes. This disturbance in redox balance was further explored by molecular level investigation. The transcriptional profiles revealed impaired oxidative phosphorylation (OXPHOS) and tricarboxylic acid (TCA) cycle pathways, which potentially inhibited the oxidative respiratory chain in fish following exposure to BaP, and reduced the production of adenosine triphosphate (ATP) and succinate dehydrogenase (SDH). Furthermore, this investigation indicated a potential connection to apoptosis, as demonstrated by fluorescence microscopy and histological analyses, and supported by an increase in the expression levels of related genes via real-time quantitative PCR. This study enhances our understanding of the molecular-level impacts of BaP's multifaceted toxicity in the early life stages of marine medaka, and the associated risks.

1. Introduction

Polycyclic aromatic hydrocarbons (PAHs) are significant pollutants originating from various sources such as petrogenic (petroleum activity), pyrogenic (incomplete combustion), diagenetic (sediment transformation), and biogenic (natural metabolic processes by microorganisms and plants) (Ahad et al., 2015; Jesus et al., 2022; Honda and Suzuki, 2020; Dhar et al., 2020). Petrogenic and pyrogenic sources are mainly anthropogenic. PAH pollution in aquatic environments occurs in two main scenarios: accidental events, such as the 2003 Tasman Spirit oil spill in Karachi (Siddiqi et al., 2009), and the 2018 East China Sea collision (Wan and Chen, 2018), and continuous introduction through daily activities like fossil fuel use, vehicular emissions, and industrial processes. These pollutants reach oceans and lakes via land runoff, urban drainage, and atmospheric deposition (Abdel-Shafy and Mansour, 2016; Pereira, 2014).

Among the diverse array of PAHs, benzo[a]pyrene (BaP) is regularly detected, making it a commonly used marker for PAH contamination (Valero-Navarro et al., 2007). BaP is commonly found in the marine environment and was identified at levels around 8.61 μg/L in an Indian river, along with other PAHs (Singare, 2016). In Zhejiang Province,

* Corresponding author.
E-mail address: wkjian@xmu.edu.cn (K.-J. Wang).

https://doi.org/10.1016/j.aquatox.2024.107016
Received 27 February 2024; Received in revised form 5 June 2024; Accepted 29 June 2024
Available online 29 June 2024

Abbreviation

sod1	superoxide dismutase 1
sod2	superoxide dismutase 2
cat	catalase (gene)
gst	glutathione S-transferase
gpx	glutathione peroxidase
sdha	succinate dehydrogenase a
sdhb	succinate dehydrogenase b
sdhd	succinate dehydrogenase d
cox1	cytochrome c oxidase subunit 1
cox4	cytochrome c oxidase subunit 4
cox6a	cytochrome c oxidase subunit 6a
cyt b	cytochrome b
ndufb11	NADH dehydrogenase (ubiquinone) 1 beta subcomplex subunit 11
atp5d	F-type *H*+-transporting ATPase subunit delta
diablo	direct IAP binding protein with low pI or second mitochondria-derived activator of caspases (SMAC)
apaf1	apoptotic Peptidase Activating Factor 1
casp3	caspase 3
casp9	caspase 9
ahr	aryl hydrocarbon receptor
hsp90a	heat shock protein alpha
cyp1a1	cytochrome p450 1a1
cyp1b1	cytochrome p450 1b1
H_2O_2	hydrogen peroxide
ROS	reactive oxygen species
MDA	malondialdehyde
T-AOC	total antioxidant capacity
SOD	superoxide dismutase
CAT	catalase (enzyme)
GST	glutathione transferase
GPx	glutathione peroxidase
SDH	succinate dehydrogenase
ATP	adenosine triphosphate
DEGS	differentially expressed genes
DMSO	dimethyl sulfoxide
DPF	day post fertilization
OXPHOS	oxidative phosphorylation
TCA cycle	tricarboxylic acid cycle

China, surface waters have BaP concentrations ranging from 1 ng/L to 1.8 μg/L (Zhu et al., 2008). Another investigation reported that BaP concentrations in seawater along the coast of China ranged from 0.001 to 4.799 μg/L in polluted zones (Su et al., 2017). These findings underscore the significance of regular assessment of the toxicological effects of BaP pollution in aquatic ecosystems. Presently, within aquatic environments, *in vivo* models serve as supplementary methods for assessing the biological consequences of pollutants (Gerbersdorf et al., 2015; Altenburger et al., 2018) Notably, the marine medaka (*Oryzias melastigma*) has gained prominence in research as a model organism for estuarine and marine ecotoxicology due to its rapid growth and development, cost-effectiveness, and various other benefits (Bo et al., 2011; Dong et al., 2014; Kong et al., 2008; Lee et al., 2018). Therefore, information regarding BaP toxicity in the marine environment can be obtained using the marine medaka as an *in vivo* model.

Fish, in their early stages, are highly vulnerable to environmental pollutants, which can cause a range of abnormalities, as documented by various studies (Huang et al., 2013; Zhao et al., 2017; Zheng et al., 2020). Regarding BaP's effects on early development, several scientific investigations utilized both marine and freshwater fish. However, concerning BaP's impact on early stages of fish, much attention and multifaceted investigations have been conducted on freshwater species, exploring various scenarios including chronic and acute exposures, as well as exposure to both high and environmental-level concentrations. Noteworthy examples of such studies include research on rainbow trout (*Salmo gairdneri Richardson*) (Hose et al., 1984), Japanese medaka (*Oryzias latipes*) (Chikae et al., 2004; Hornung et al., 2007; Pannetier et al., 2019; Yamaguchi et al., 2020), and zebrafish (*Danio rerio*) (Corrales et al., 2014; Elfawy et al., 2021; Huang et al., 2015, 2012; Incardona et al., 2011; Knecht et al., 2017; Lin et al., 2020). However, findings from these freshwater studies may not directly apply to marine environments due to differing ecological characteristics. Research suggests that contaminants behave differently in seawater compared to freshwater (Wu et al., 2012; Kang et al., 2008).

Conversely, previous studies on marine fish species during early life stages have largely focused on particular facets, with most investigations involving short-term exposure to high concentrations of BaP. For example, studies on killifish (*Fundulus heteroclitus*) investigated CYP1A inhibition, heart deformities, and liver toxicity across BaP exposures ranging from 10 to 400 μg/L (Wang et al., 2006; Wills et al., 2010, 2009). Study on marine medaka explored the whole cytochrome P450 system, with effective concentrations observed at 10 and 100 μg/L BaP (Kim et al., 2014). Additionally, marine medaka embryos showed significant induction of EROD and Caspase-3/7 activities at low BaP doses after 8-days exposure (Lin et al., 2011). At 20 μg/L BaP, Mu et al. (2012) reported a significant drop in the hatching rate, while another study observed a delay in hatching time following exposure to 200 μg/L BaP in marine medaka (Sun et al., 2020). Research on red seabream (*Pagrosomus major*) investigated developmental toxicities following 48-hour BaP exposure (Zhao et al., 2017). Investigations on rockfish (*Sebastiscus marmoratus*) and milkfish (*Chanos chanos*) found that short-term BaP exposure led to neurotoxic effects (He et al., 2012; Palanikumar et al., 2012). Furthermore, exposure of marine medaka (*Oryzias javanicus*) to 10 and 20 μg/L BaP for one week resulted in oxidative damage, while malformations in embryos were detected at concentrations of 5 μg/L BaP and above (Nam et al., 2020). However, there is still a gap in fully capturing the multifaceted potential impacts of BaP on marine fish early life stages under chronic exposure to environmentally relevant concentrations. Relying on short-term studies may underestimate its effects, particularly at the concentrations available in the environment. Therefore, there is a need to enhance our understanding of its diverse hazard potential. Our study addresses these gaps by evaluating developmental abnormalities, growth disruptions, histological alterations, oxidative stress, biochemical equilibrium, and molecular changes. This comprehensive approach provides valuable insights into the early developmental stages and environmental risks associated with BaP exposure in marine fish.

2. Material and methods

2.1. Chemical and reagents

New stocks of BaP with a purity of at least 96 % (CAS # 50–32–8), and tricaine methanesulfonate (MS-222) were acquired from Sigma-Aldrich (Shanghai, China). Dimethyl sulfoxide (DMSO) meeting the specifications for molecular biology with a purity level of at least 99 % was sourced from Sangon Biotech (Shanghai, China). DMSO was used to dissolve BaP and formulate stock solutions (1, 3, and 5 mg/mL). These stock solutions were used throughout the experiment to prepare the required BaP concentrations of 1, 4, and 8 μg/L. In the examination of both the control and treatment solutions, sets of samples ($n = 3$) were collected, and analyses were conducted using a fluorescence

spectrophotometer (Cary Eclipse, Varian, USA). The corresponding values are detailed in Table S3. The procedure followed the method described in our previous study (Bo et al., 2014; Yin et al., 2020). Notably, the BaP concentrations measured in the blank (seawater) and solvent (DMSO) control samples were undetectable. As no statistically significant differences were observed in the data from the solvent control group compared to the blank control, we opted to include only the solvent control group for simplicity in this study.

2.2. Animal ethics

The handling of fish experiments strictly followed the regulations outlined by the National Institute of Health Guidelines for the Care and Use of Laboratory Animals. The animal research protocol was approved by the animal welfare and ethics committee of Xiamen University.

2.3. Marine medaka maintenance and exposure assay

Breeding was initiated by placing 200 healthy males and females per tank (5 replicates) overnight, under conditions of a constant temperature of 27 ± 1 °C, salinity of 28 ± 2 %, and a light cycle of 14 h of light followed by 10 h of darkness. The following morning, eggs were gathered one hour after the lights were switched on. Embryos were rinsed three times with water devoid of chemicals and subsequently placed in glass petri dishes containing artificial saltwater. Only fertilized eggs at the same developmental stage were chosen for exposure experiments after examination under a dissecting microscope. Approximately 5000 fertilized embryos were randomly grouped into sets of 200 each and assigned to the control and three treatment levels: 1, 4, and 8 μg/L of BaP. These concentrations were chosen based on their relevance to aquatic environments (Singare, 2016; Su et al., 2017; Zhu et al., 2008). Preliminary exposure experiments considered concentrations of 0.1, 0.5, 1, 4, and 8 μg/L BaP, revealing that concentrations below 1 μg/L BaP showed no significant morphological and biochemical responses in embryonic and larval stage (data not shown). The study proceeded using the remaining three concentrations of BaP and a solvent control (DMSO). Each treatment comprised five replicate groups, with three replicates used as biological replicates and the remaining two serving as backups. All the treatment and solvent control groups received a constant DMSO concentration of < 0.001 % (v/v). After hatching, approximately 100 larvae were transferred to 15 L tanks, with each tank containing 12 L of the exposure solution. They remained in this environment until 30 days post fertilization (dpf). Feeding began daily from the 15 dpf stage onward. Throughout the 30-day exposure period, the water was changed daily, the BaP in each tank was renewed, and the embryos were inspected and photographed daily using a Leica DMi1 inverted microscope (Leica, Germany) fitted with a Leica DMC4500 digital microscope camera. Any deceased embryos displaying whitening were removed daily.

2.4. Effects of bap on larval medaka

Daily monitoring was performed to assess the BaP effects, including hatching rate, timing, mortality, and heartbeat rate. Hatching rate (%) was calculated as the number of successfully hatched larvae / initially stocked embryos × 100. Larval mortality rate calculated as (total number of dead larvae / initially hatched larvae) × 100. The heartbeat frequencies of embryos ($n = 10$) were enumerated in three distinct sets of replicates using automatically recorded 30-second videos with a Leica DMi1 inverted microscope equipped with a camera. For biometric measurements and encompassing anomalies, randomly selected larvae ($n = 5$) from each replicate were anesthetized using 0.02 % MS-222, placed in a chamber containing 3 % methylcellulose, and photographed using a stereomicroscope equipped with an Mshot MS 60 camera (Guangzhou, China). Anomalies were classified by microscopic examination, following the procedures outlined by Cong et al. (2017) and Li et al. (2020). Total body length was measured using the Mshot image analysis software, with the scale bar adjusted to millimeters (mm). Weight was measured using a digital weighing scale.

2.5. Histological analysis

At 30 dpf, marine medaka larvae ($n = 3$ / group) were immersed in 10 % buffered formalin for preservation over a 24-hour period. They underwent a gradual ethanol dehydration process, followed by xylene clearing, and were later incorporated into paraffin. Afterwards, 5 μm-thick sections were prepared and subjected to hematoxylin and eosin (HE) staining for microscopic examination. An optical upright microscope, the Leica DM2500 LED, equipped with a DFC7000 T camera, was used for examination. The analysis was performed using Leica Application Suite X 3.7.2.22383, ©2020 software. Three different magnifications (10x, 20x, and 40x) were used for each sample to obtain a closer view of the liver.

2.6. Measurement of oxidative parameters

Tissue homogenates were prepared by pooling 10 larvae as a sample ($n = 6$), homogenized in cold saline at a concentration of 10 % (w/v) using an electric homogenizer (Tiangen Biotech, China). The resulting supernatants were collected after centrifugation at 3500 g for 10 min at 4 °C. Hydrogen peroxide (H_2O_2), malondialdehyde (MDA), superoxide dismutase (SOD), catalase (CAT), glutathione S-transferase (GST), glutathione peroxidase (GPx), and total antioxidant capacity (T-AOC) were measured at 405, 532, 520, 412, 412, and 240 nm, respectively. Reactive oxygen species (ROS) content was assessed using chemiluminescence with excitation at 502 nm and emission at 530 nm. Readings were taken using a spectrophotometer (Agilent Technologies, Cary 60 UV–Vis, USA) and Tecan microplate reader (Infinite F200 Pro, Switzerland). All kits were sourced from Nanjing Jiancheng Bioengineering Institute, China. Protein concentration in each sample was quantified using the Pierce BCA Protein Assay Kit (Thermo Scientific, USA), with a standard curve derived from the BCA protein determination method.

2.7. Measurement of ATP assay and SDH

Succinate dehydrogenase (SDH) activity was determined in 10 % tissue homogenates using an SDH assay kit, following the instructions provided by the manufacturer. Readings were taken at an optical density (OD) value of 600 nm at 5 s (OD1) and again at 65 s (OD2) after a 1-minute wait. Adenosine triphosphate (ATP) content was evaluated using an ATP assay kit. ATP concentration was determined in the tissue homogenate by measuring the OD at 636 nm based on a color formation reaction involving creatine and ATP catalyzed by creatine kinase. Both the SDH and ATP kits were obtained from the Nanjing Jiancheng Bioengineering Institute, China, and measurements were taken in triplicate.

2.8. AO staining for apoptosis

Acridine orange (AO) was used to assess apoptosis in medaka larvae ($n = 5$/group) from both the control and BaP-treated groups (1, 4, and 8 μg/L). The larvae were washed twice with filtered fish medium. AO (5 μg/mL), dissolved in fish medium, stained the larvae in the dark for 20 min, followed by two 5-minute washes to remove excess stain. The fish were immobilized with MS-222 salt, positioned laterally, and mounted on 3 % methylcellulose for imaging using the green channel of an Axis Observer A1 inverted fluorescence microscope (Zeiss, Germany) to evaluate apoptosis.

2.9. Isolating RNA and sequencing the transcriptome

TRIzol Reagent (Invitrogen, USA) was used to extract total RNA from

larval medaka in the control and exposure groups (1, 4, and 8 μg/L BaP), in accordance with the guidelines provided by the manufacturer. Each sample consisted of a blend of five larvae with three replicates each. A Nanodrop 2000 microvolume spectrophotometer (Thermo Fisher Scientific, USA), and an Agilent 2100 bioanalyzer (Agilent Technologies, USA) were used to evaluate RNA quantity and integrity. Gel electrophoresis (1.2 % agarose) was used to verify degradation and contamination. RNA samples (1 μg/L BaP and control) were prepared using the NEBNext® Ultra™ RNA Library Prep Kit for Illumina® (NEB, USA) at Novogene Bioinformatics Technology Co., Ltd., China. The exposure concentration of 1 μg/L BaP was selected for RNA-seq because it represents the most commonly detected level in the environment and the lowest concentration in our study, with the aim of investigating transcriptional regulation at the lowest feasible level. Sequencing was performed using an Illumina HiSeq platform to produce paired-end reads. The DEGseq R package (version 1.10.1) was used to analyze differential expression. *P*-values were adjusted using the *q*-value to identify differentially expressed genes (DEGs) with a threshold *q*-value < 0.005 and $|\log2(\text{fold-change})| > 1$(Storey and Tibshirani, 2003). Gene Ontology (GO) enrichment analysis of DEGs was performed using the GOseq R package (Young et al., 2010), accounting for gene length biases. DEGs in Kyoto Encyclopedia of Genes and Genomes (KEGG) pathways were assessed using KOBAS software (Mao et al., 2005). The sequencing data have been submitted to the Sequence Read Archive at the National Center for Biotechnology Information (NCBI) under accession code PRJNA1119179.

2.10. Analysis of real-time quantitative PCR (RT-qPCR)

RNA was acquired using the TRIzol method and used to synthesize cDNA via reverse transcription using the PrimeScript RT Reagent Kit (TaKaRa, China). Primer sequences were tailored using NCBI/Primer-BLAST or obtained from our previous research (Table S1). Dissociation analysis and standard curves validated primer specificity and amplification efficiency (95–105 %). The Fast-Start SYBR Green PCR Master Mix (Roche, USA) and ABI 7500 system were used for quantitative PCR assays, involving cycling conditions commencing at 95 °C for 10 min, followed by 40 cycles at 95 °C for 30 s and 60 °C for 1 min. Each group included three biological replicates, and three operational replicates were performed for each sample. For data normalization, *18 s* gene was used as a reference to determine the expression levels of the target genes using the $2^{-\Delta\Delta CT}$ method (Livak and Schmittgen, 2001).

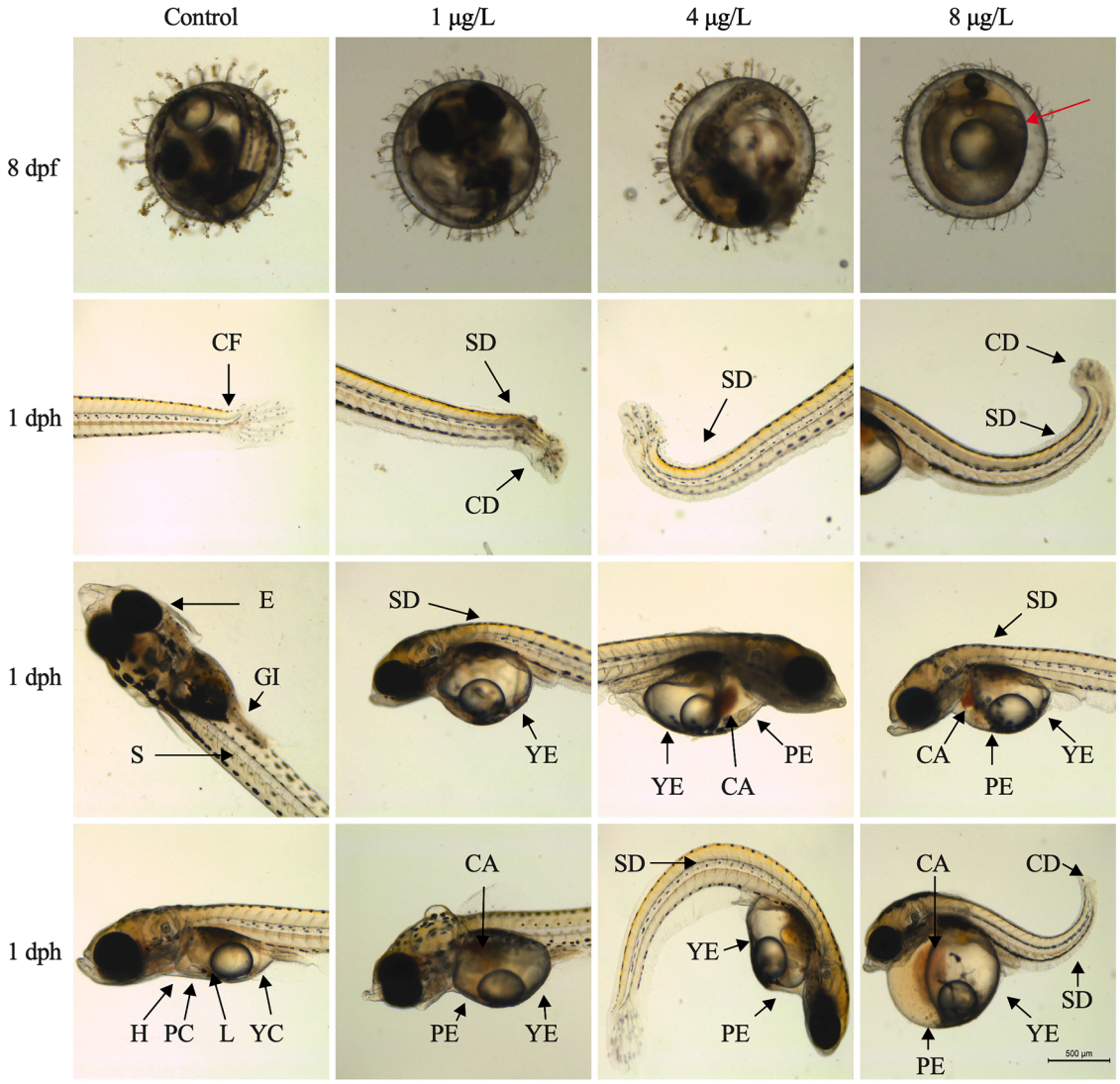

Fig. 1. The morphology of marine medaka larvae and embryos exposed to 1, 4, and 8 μg/L BaP. Red arrows highlight the defective embryo. Key labels: H - heart; L - liver; PC - pericardium; YC - yolk sac; GI - gastrointestinal tract; S - spine; E - eyes; YE - yolk sac edema; PE - pericardial edema; CA - cardiac anomalies; SD - spinal deformities; CD - caudal fin deformities. Scale bar = 500 μm.

2.11. Statistical analysis

Larvae images were arranged using Adobe Photoshop. Data analysis and graph generation were performed using GraphPad Prism 7.0 (GraphPad Software, USA). Results are presented as mean (M) ± standard deviation (SD). Data sets were assessed for normality and homogeneity using the Kolmogorov-Smirnov or Shapiro-Wilk normality tests prior to conducting ANOVA. Differences between the control and BaP-treated groups were analyzed using one-way ANOVA, followed by Dunnett's multiple comparison test. Statistical significance is indicated by $*p < 0.05$, $**p < 0.01$, and $***p < 0.001$ compared with the control group.

3. Results

3.1. Effects of BaP on morphological and physiological aspects

BaP exposure resulted in various abnormalities in medaka larvae, including pericardial and yolk-sac edema, skeletal deformities, and cardiac anomalies (Fig. 1; Fig. S2-S6). These malformations were observed in all three BaP-exposed groups (1, 4, and 8 µg/L BaP) compared to the control, with percentages of 16.33, 18, and 22.67 %, respectively (Table S4). The hatching rate of medaka embryos decreased to 74 %, 65 %, and 56 % in the 1, 4, and 8 µg/L BaP groups, respectively (Fig. 2A). Additionally, there was a delay of 1 day in the 1 µg/L BaP group and 2 days in the 4 and 8 µg/L BaP groups for the first hatch compared to the control. As the concentration of BaP increased, the survival rate decreased (Fig. 2B and Table S4). A notable reduction in the heartbeat rate, reaching statistical significance ($p < 0.05$), was

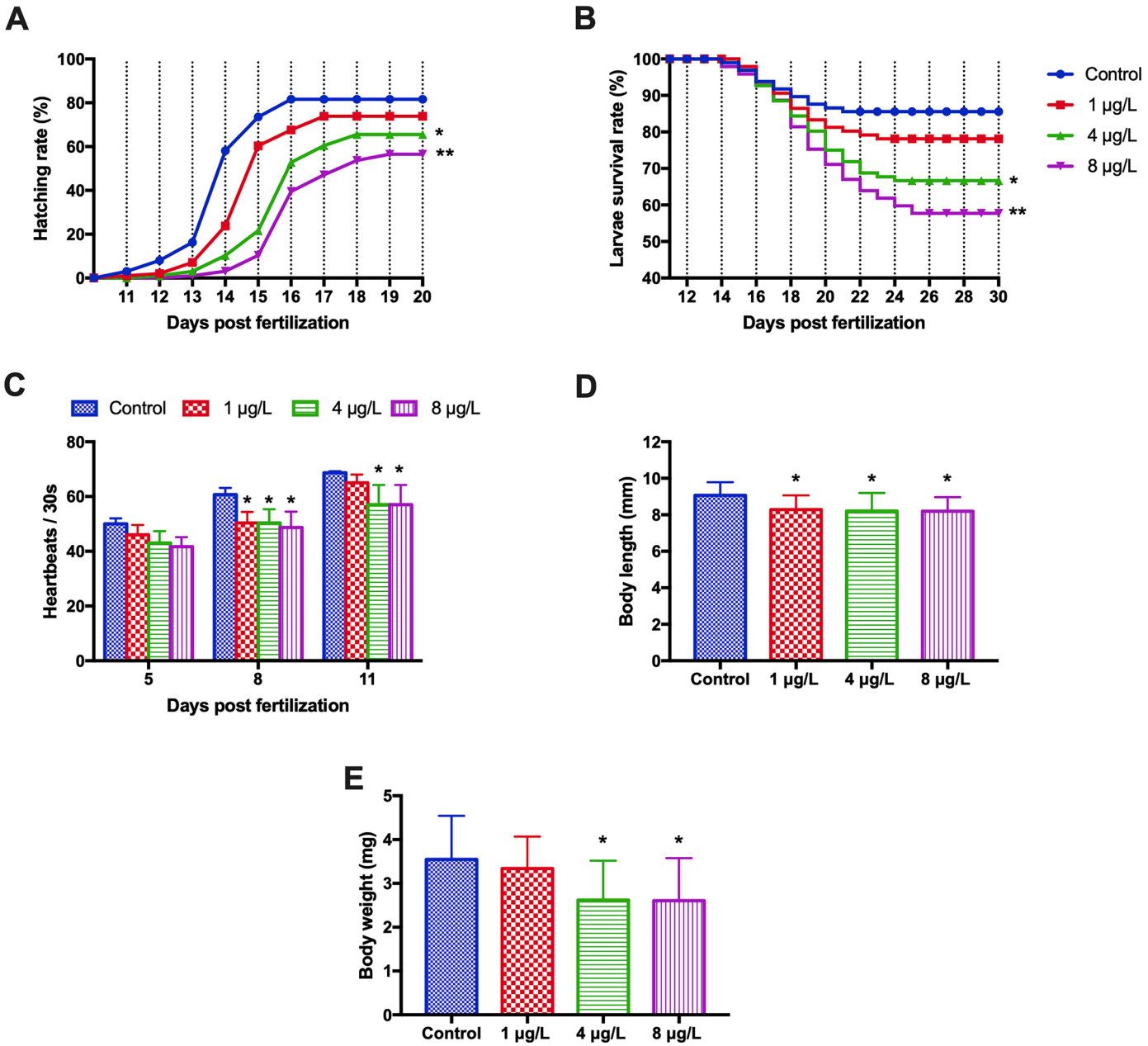

Fig. 2. Hatching rates (A), larval survival rate (B), heartbeats (C), body length (D), and body weight of larvae at 30 dpf (E) following exposure to 1, 4, and 8 µg/L BaP. The mean ± SD (standard deviation) is utilized to represent the data. Significant distinctions between the exposure and control groups are manifested at $*p < 0.05$, and $**p < 0.01$.

observed in the BaP-exposed groups, particularly at the 4 and 8 μg/L concentrations (Fig. 2C). Moreover, after the 30-day exposure period, the body length was significantly reduced ($p < 0.01$) in all BaP-exposed groups (Fig. 2D). In contrast, body weight showed significant differences ($p < 0.01$) in 4 and 8 μg/L BaP groups, whereas the 1 μg/L BaP group did not exhibit significant difference (Fig. 2E; Table S4).

3.2. Effects of BaP on hepatic histomorphology

The control group displayed healthy liver histology with well-defined blood sinusoids, hepatocytes, and standard hepatocyte staining. However, BaP-treated larvae exhibited apparent hepatic damage compared to healthy control livers (Fig. 3), such as loss of cytoplasmic details, empty intercellular spaces, swollen hepatocytes, loss of cellular details, and the presence of densely stained structures known as karyolysis (disintegration of the cell nucleus). Additionally, certain hepatocytes exhibited a lighter and irregular staining pattern with H&E, particularly in the 8 μg/L BaP group.

3.3. Effects of BaP on oxidative parameters

BaP exposure significantly increased ROS levels ($p < 0.02$, < 0.001) in the 1, 4, and 8 μg/L BaP groups, respectively, compared to the control (Fig. 4A). Exposure to 4 and 8 μg/L BaP significantly increased H_2O_2 levels ($p < 0.04$, < 0.01), respectively, while 1 μg/L BaP did not induce a statistically significant difference (Fig. 4B). Additionally, MDA levels increased substantially ($p < 0.02$, < 0.01, < 0.004) in response to 1, 4, and 8 μg/L BaP treatment, respectively (Fig. 4C). Further, BaP significantly decreased the activity of SOD ($p < 0.04$, < 0.02, and < 0.003) in the 1, 4, and 8 μg/L groups, respectively, demonstrating a distinct contrast with the control groups (Fig. 4D). CAT activity was reduced in all three groups exposed to BaP ($p < 0.04$, < 0.008, and < 0.008) at 1, 4, and 8 μg/L, respectively (Fig. 4E). Regarding GST activity, a substantial decrease ($p < 0.02$, < 0.006) was noted in the 4 and 8 μg/L BaP-treated groups compared to the control group (Fig. 4F). GST activity in the 1 μg/L BaP-treated group did not show any noticeable changes. However, GPx activity was significantly different ($p < 0.03$) among all BaP-exposed groups (Fig. 4G). BaP markedly reduced the levels of T-AOC at higher doses ($p < 0.03$, < 0.008) at 4 and 8 μg/L, whereas no significant difference was observed at 1 μg/L (Fig. 4H).

3.4. Effects of BaP on SDH and ATP concentration

BaP reduced SDH activity in larval medaka and exhibited substantial alterations with significant values ($p < 0.02$, < 0.01, < 0.006) in groups treated with 1, 4, and 8 μg/L of BaP, respectively (Fig. 5A). Additionally, significant reductions in ATP content were observed in the BaP-exposed groups (1, 4, and 8 μg/L), with values of $p < 0.03$, < 0.02, and < 0.006, respectively (Fig. 5B).

3.5. Transcriptomic profiling and altered pathway dynamics

Exposure to BaP significantly altered gene transcription in medaka larvae, leading to the identification of 2679 differentially expressed genes (DEGs). Among these, 615 DEGs were upregulated, and 2064 DEGs were downregulated (Fig. 6A; Fig. S7A). The results of the quality assessment of the sequenced samples are presented in Table S4. Functional enrichment analysis identified 831 DEGs associated with molecular function (MF), 1781 with biological processes, and 410 with cellular components (CC) (Fig. S7B). The analysis of DEGs through KEGG pathway enrichment identified the top 20 significantly enriched pathways, each pathway containing more than 10 DEGs, with a p-value < 0.05 (Fig. 6B; Table S5). The majority of the DEGs were associated with pathways related to oxidative metabolism and detoxification. Among these, the oxidative phosphorylation (OXPHOS) pathway exhibited the highest number of DEGs, totaling 65, and 19 DEGs

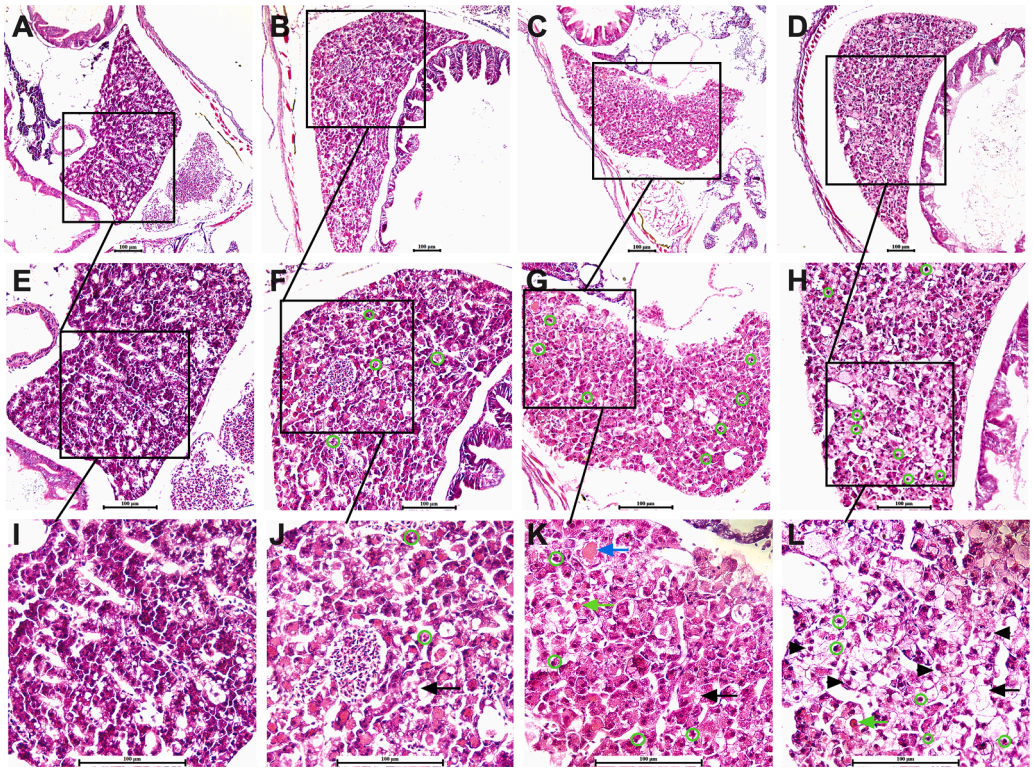

Fig. 3. Histological changes in the livers of marine medaka larvae. Control (A, E, I), 1 μg/L exposure (B, F, J), 4 μg/L exposure (C, G, K), and 8 μg/L exposure (D, H, L). Loss of cytoplasmic inclusions (green circle), empty intercellular spaces (black arrow), swollen hepatocytes (arrowheads), loss of cellular details (blue arrows), and karyolysis (green arrows). The microscopic images are magnified 10x, 20x, and 40x their original size, from top to bottom, respectively.

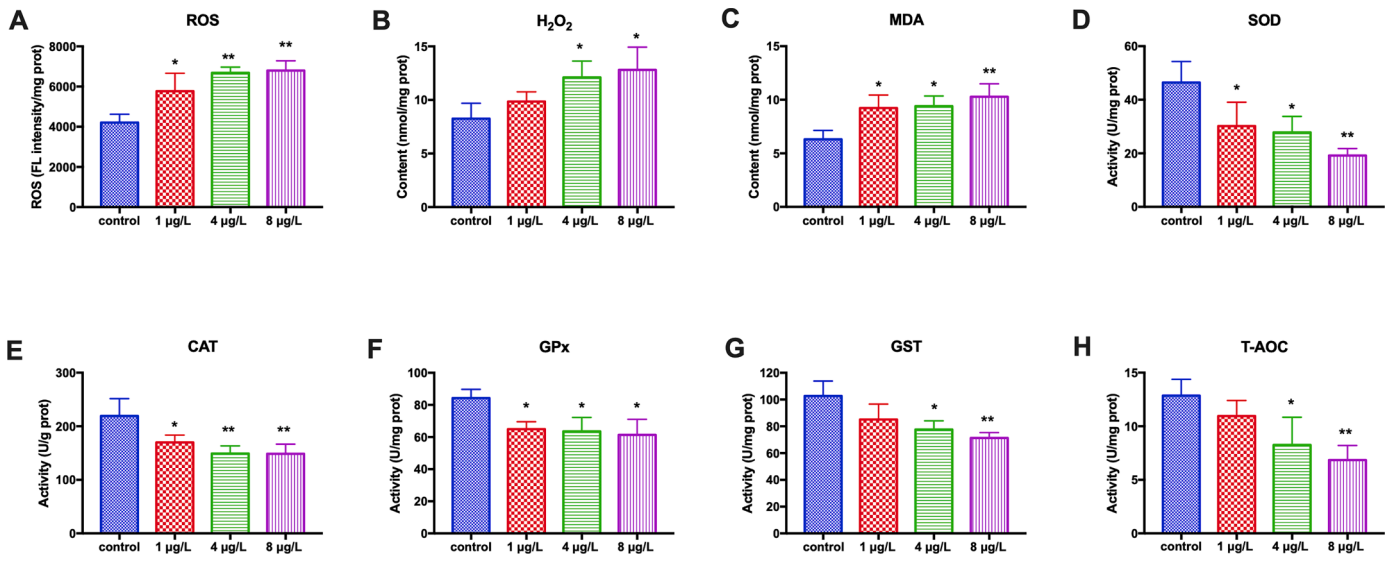

Fig. 4. BaP impact on the oxidative stress response. ROS (A), H_2O_2 content (B), MDA content (C), SOD activity (D), CAT activity (E), GPx activity (F), GST activity (G), and T-AOC content (H) activity in marine medaka larvae after exposure to 1, 4, and 8 μg/L BaP. The mean ± SD (standard deviation) is utilized to represent the data. Significant distinctions between the exposure and control groups are manifested at $^*p < 0.05$, and $^{**}p < 0.01$.

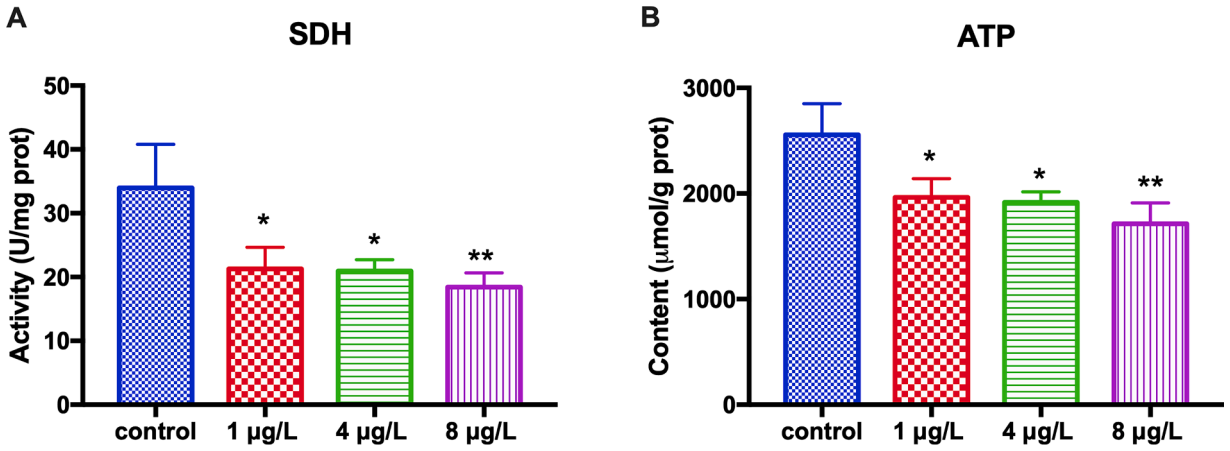

Fig. 5. Effects of BaP on SDH and ATP activities. SDH activity (A), ATP content (B) in marine medaka larvae following 1, 4, and 8 μg/L BaP exposure. The mean ± SD (standard deviation) is utilized to represent the data. Significant distinctions between the exposure and control groups are manifested at $^*p < 0.05$, and $^{**}p < 0.01$.

appeared in the tricarboxylic acid (TCA) cycle pathway (Fig. 6C). To further validate the transcriptomic findings, we conducted qPCR analysis on genes associated with OXPHOS and TCA cycle pathways (*ndufb11, sdha, sdhb, sdhd, cytb, cox1, cox4, cox6a, and atp5d*) (Fig. S8C), as well as genes involved in metabolism and detoxification (*ahr, hsp90a, cyp1a1, cyp1b1, sod1, sod2, cat, gst, and gpx*) (Fig. S8A, and B). The qPCR results corroborate the trends observed in the transcriptomic data, enhancing the reliability of our findings.

3.6. Apoptotic responses elicited by BaP in medaka larvae

Apoptosis assessment in medaka larvae was performed using fluorescence microscopy with AO staining and qPCR for gene analysis. As shown in Fig. 7C, green fluorescence intensity increased with increasing BaP concentration. Apoptotic cells, marked by green dots, were widespread, especially in the head and backbone areas of the BaP-exposed medaka larvae. To investigate the gene responses associated with apoptosis, the mRNA levels of specific apoptotic genes, including *diablo, apaf1, casp9*, and *casp3*, were analyzed. The *diablo* mRNA levels exhibited a significant increase, correlating with the BaP exposure concentration in the treated groups compared to the controls. The *p*-values were < 0.006 for 1 μg/L and < 0.0001 for both 4 μg/L and 8 μg/L (Fig. 7C; Fig. S9A). *Apaf1* mRNA levels increased significantly in the same manner in the 4 and 8 μg/L BaP-treated groups ($p < 0.01$) (Fig. 7C; Fig. S9B). *Casp9* and *casp3* displayed a comparable pattern, showing a significant increase in mRNA levels in the groups exposed to 4 and 8 μg/L BaP, with *p*-values of < 0.04 and < 0.005 for *casp9*, and < 0.01 for *casp3* in both concentrations, respectively (Fig. 7C; Fig. S9C and D). Nevertheless, there were no statistically significant alterations in *apaf1, casp9*, and *casp3* expression between the 1 μg/L BaP-exposed and control groups (Fig. 7C; Fig. S9).

4. Discussion

This study revealed that concentrations of BaP, equivalent to those found in the environment, induced significant toxicity during the early developmental stages of marine medaka. Even at the low level of 1 μg/L, chronic BaP exposure resulted in abnormal development and deformities, confirming the detrimental effects of BaP at modest concentrations.

It is well known that BaP exposure results in a decrease in the hatching rate and a delay in the hatching of fish embryos (Chikae et al.,

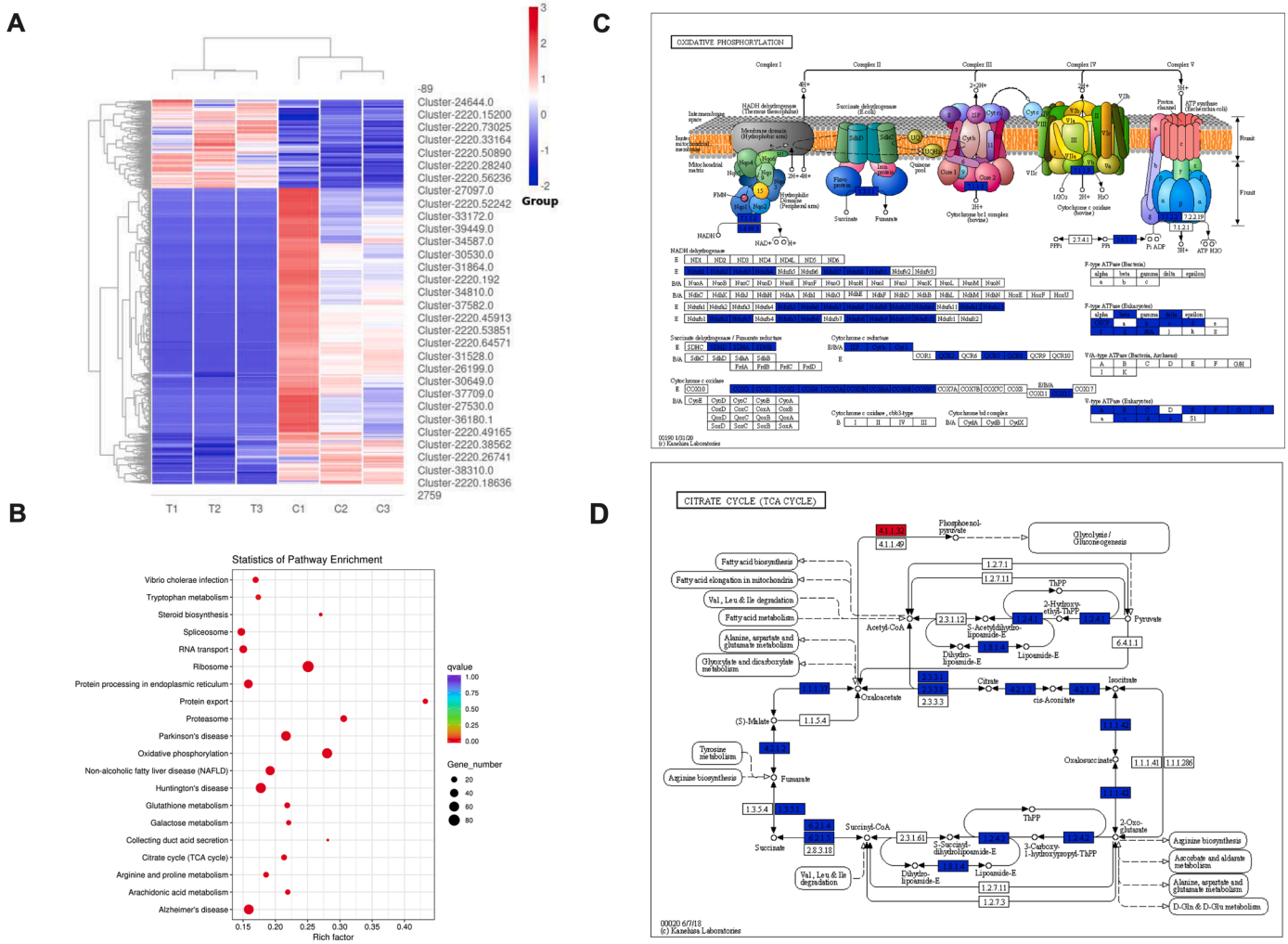

Fig. 6. Overview of the transcriptome in marine medaka larvae following exposure to BaP. Heat map showing cluster analysis of gene expression patterns for common DEGs in control *vs* exposed groups ($n = 3$) (A). KEGG enrichment pathways of DEGs. Bubble size represents the number of genes, and color indicates the p-values (B). The illustration of the enrichment of genes in the oxidative phosphorylation pathway (C) and TCA cycle (D). Blue shading highlights genes that exhibit differential expression.

2004; Fang et al., 2013; Sun et al., 2020) (Table S6). Our results align with these previous findings, showing a significant decrease and delay in the hatching rate after BaP exposure. The delay in hatching makes embryos more vulnerable to predators, endangering the continuation of the fish population. Furthermore, BaP exposure in this study induced noticeable edemas, motionless blood clots in larvae, and significantly decreased heartbeat rates in all exposure groups, indicating cardiotoxicity. Cardiotoxicity during the early stages of fish development due to BaP exposure has been identified in various studies (Huang et al., 2012; Wills et al., 2009; Yamaguchi et al., 2020). In young fish, the heart, one of the first organs to form, plays a crucial role in embryo survival and development, rendering them more vulnerable to cardiotoxicity than adults due to their small size and immature detoxification pathways (Incardona and Scholz, 2017). It is presumed that poor heart function might contribute to the malformations observed during early development in this study. Additionally, in our 30-day BaP exposure study, marine medaka larvae exhibited significantly lower body weight and length. BaP has been associated with growth retardation and reduced biometric measures (Albornoz-Abud et al., 2021; Elfawy et al., 2021). According to Mayer et al. (2018), disruptions in metabolic pathways caused by xenobiotics can lead to increased energy demands and consequent decreases in body weight. Our findings suggest that medaka larvae may have undergone considerable metabolic strain in detoxifying BaP, resulting in diminished body weight and length. Hence, in our study, we assume that a poor detoxification mechanism might be one reason for the observed differences in biometric measurements and cardiac anomalies, potentially resulting in higher mortality rates and deformities.

To explore further about the toxicity of BaP in early stages, we measured oxidative stress and antioxidant responses following BaP exposure. MDA serves as a practical parameter for assessing oxidative stress due to its simplicity and effectiveness as a biomarker (Tsikas, 2017). MDA is closely linked with the formation of ROS, and in our study, both MDA and ROS levels exhibited a significant increase alongside H_2O_2 levels. The antioxidative system plays a crucial role in the detoxification metabolism of BaP. SOD actively converts superoxide anions to hydrogen peroxide with the assistance of CAT and GPx, ultimately transforming it into water and oxygen (He et al., 2017). Additionally, the GST enzyme aids in detoxifying toxic BaP metabolites, converting them into less harmful products that can be eliminated from the body (Trushin et al., 2012). T-AOC encompasses more than just the summation of individual antioxidant measures, including those yet to be discovered (Ghiselli et al., 2000). In this study, we observed significant decreases in the activities of antioxidant enzymes as well as in mRNA expression levels of *sod1, sod2, cat, gpx,* and *gst* in all BaP-exposed larval medaka. The reduced activity of antioxidants, coupled with elevated

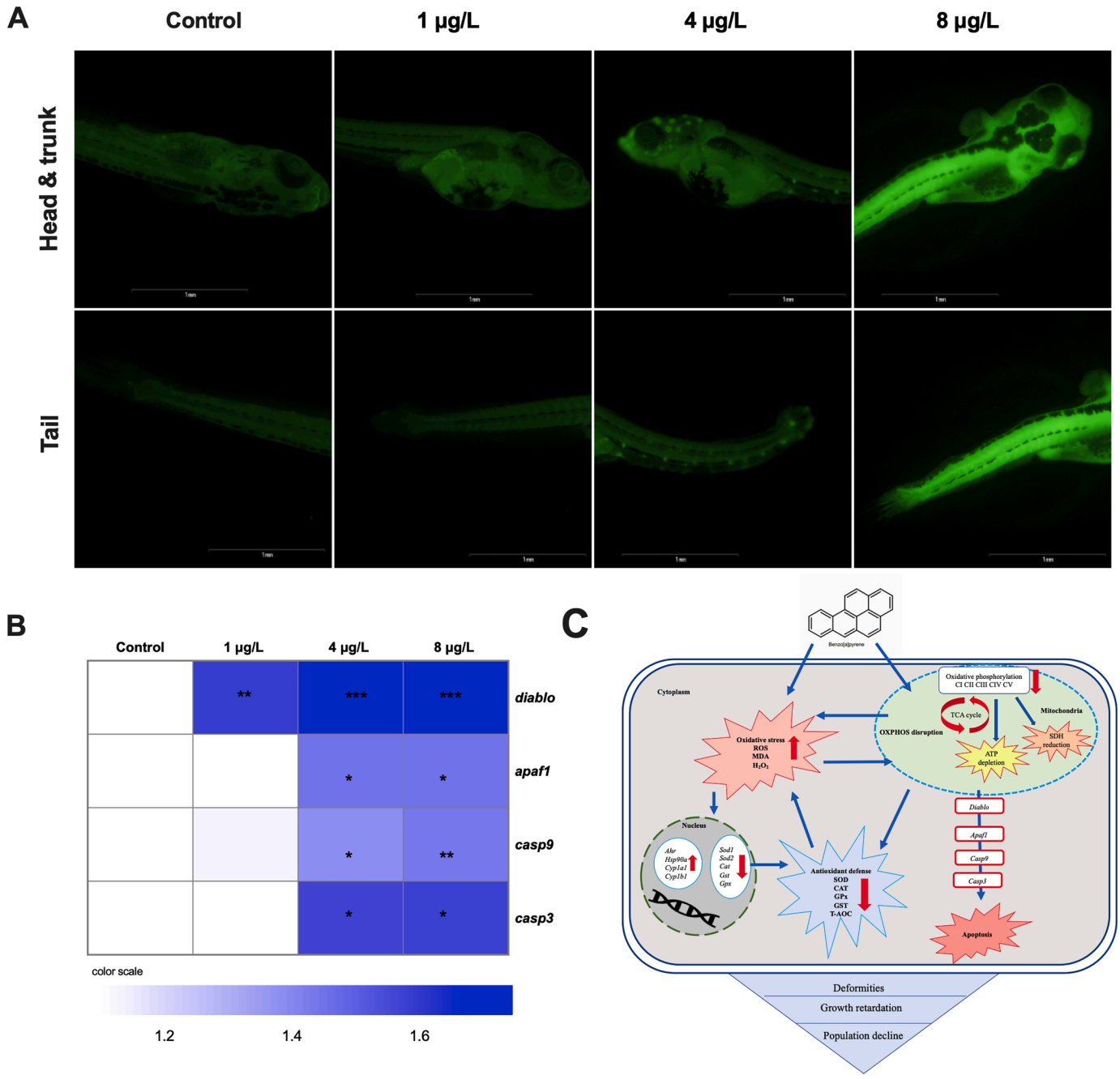

Fig. 7. The figure illustrates the effects of BaP on apoptosis. AO staining of control and BaP-exposed medaka larvae revealed a pronounced increase in green fluorescence, particularly at high concentrations of BaP (A). The heat map presents relative mRNA levels of genes in marine medaka larvae associated with apoptosis after 1, 4, and 8 µg/L BaP exposure (B). A schematic diagram illustrates the proposed BaP-induced toxicity mechanism in marine medaka larvae (C). The mean ± SD (standard deviation) is utilized to represent the data. Significant distinctions between the exposure and control groups are manifested at $^{*}p < 0.05$, $^{**}p < 0.01$, and $^{***}p < 0.001$.

levels of oxidants, suggests an imbalance in the redox status induced by BaP exposure. The decrease in antioxidant activities implies a weakened antioxidant defense, thereby heightening the risk of oxidative damage and associated consequences. Similar disturbances in antioxidant defense due to chronic BaP exposure have been reported in rats by Sheweita et al. (2016). Conversely, some studies have reported elevated levels of antioxidants in fish in response to acute BaP exposure (Deng et al., 2018; Guo et al., 2021; Kim et al., 2014). Additionally, Nam et al. (2020) found that in the early stages of fish, a week exposure to 1 µg/L BaP concentration enhanced antioxidant activities, while higher concentrations decreased them. However, in our study, even 1 µg/L BaP decreased antioxidant levels, possibly due to the longer exposure duration. These results suggest that not only higher concentrations but even low levels of BaP can harm the antioxidant defense system after chronic exposure. Thus, the observed high mortality, malformations, and growth retardation are likely due to a weakened antioxidant defense.

To expand our understanding of the molecular impact of BaP on larval medaka, we conducted transcriptome analyses comparing the BaP-exposed group with the control group. The results revealed that the majority of genes were associated with oxidative metabolism, encompassing the OXPHOS and TCA cycle pathways. The OXPHOS system is integrated into the mitochondrial inner membrane and consists of five multiprotein enzyme complexes designated as (I–V). This system

primarily functions by orchestrating electron and proton transport, leading to ATP synthesis (Smeitink et al., 2001). In the mitochondrial matrix, the TCA cycle supplies electron carriers to the electron transport chain through complexes I and II, respectively (Nolfi-Donegan et al., 2020). The regulation of the TCA cycle and its continuous interaction with OXPHOS are crucial for maintaining cells in a stable state (Martínez-Reyes and Chandel, 2020). In this study, within the context of the OXPHOS pathway, multiple genes linked to the NADH dehydrogenase complex experienced significant down-regulation. Moreover, genes encoding components of succinate dehydrogenase, such as *sdha, sdhb,* and *sdhd,* were notably suppressed. Additionally, genes responsible for encoding cytochrome c reductase and cytochrome c oxidase subunits also displayed marked suppression (Fig. 6C). These findings indicate a potential inhibition of the oxidative respiratory chain in fish following exposure to BaP. A similar inhibition of the OXPHOS pathway was observed in the early life stages of Staghorn coral (*Acropora hyacinthus*) exposed to BaP (Xiao et al., 2018). Moreover, the down-regulation of NADH dehydrogenase impedes ATP production, while reduced *sdha* levels limit succinate dehydrogenase activity, resulting in disrupted biological functions. To further strengthen our understanding, we measured the ATP content and SDH enzyme activity. SDH is a unique enzyme that links the TCA cycle to OXPHOS (Moosavi et al., 2019). Our study revealed a significant reduction in both ATP content and SDH activity in marine medaka larvae following BaP exposure. This observation strongly suggests that the depletion of ATP and SDH resulted from the disruption of the OXPHOS and TCA cycles. Therefore, it's plausible that exposure to BaP triggers changes in genes associated with OXPHOS and the TCA cycle pathways, resulting in diminished activities, directly impacting ATP production and SDH activity, contributing to increased oxidative stress and disrupting crucial biological processes like compromised antioxidant activities, potentially leading to a spectrum of abnormalities.

Excessive oxidative stress, as reported by other researchers, has the potential to induce the release of cytochrome c, binding to *apaf1* and ultimately triggering cell apoptosis (Deng et al., 2009; Jin et al., 2011). In our investigation, apoptosis in larval medaka was identified through the upregulation of the *diablo, apaf1, casp9,* and *casp3* genes. *Diablo,* also known as *smac*, stimulates apoptosis by triggering caspase activation and inhibiting antiapoptotic proteins (Du et al., 2000; Redza-Dutordoir and Averill-Bates, 2016). The activation of *apaf1* is linked to pro-caspase-9, resulting in the subsequent activation of *caspase-9*, which culminates in the activation of *caspase-3*, a pivotal executor in the cellular apoptosis process (Cao et al., 2018; Lin, 1999). In this study, the imbalance in redox homeostasis, along with the inhibited OXPHOS and TCA cycle pathways, was identified as the primary factors intensifying oxidative stress and triggering apoptosis. Consequently, our hypothesis regarding apoptosis gains further support from fluorescence microscopy analysis, and histological observations revealing liver damage, indicating hepatocyte impairment in larval medaka following exposure to BaP.

5. Conclusion

This study revealed that chronic BaP exposure at environmentally equivalent levels in marine medaka during their early life stages induced multifaceted toxic effects. BaP's lethality manifested in low hatching rates, high malformation rates, and stunted growth of medaka larvae. Our comprehensive investigation delved into the biochemical and molecular damage inflicted by BaP, elucidating its potential toxicity mechanism involving redox imbalances characterized by elevated oxidants and diminished antioxidants, alongside disrupted OXPHOS and TCA cycle pathways. Consequently, ATP depletion and reduced SDH activity ensued. The disruption of molecular interactions, coupled with induced redox imbalances, culminated in apoptosis, ultimately leading to adverse effects on fish development, as depicted in Fig. 7C. While our study sheds light on the early life stages of marine medaka, it may not fully capture the entirety of BaP's effects on the fish life cycle. Future research should explore BaP's impact on other life stages, adaptation mechanisms, and sex-specific responses to gain a more comprehensive understanding of its long-term effects.

CRediT authorship contribution statement

Rabia Zeb: Conceptualization, Methodology, Data curation, Software, Writing – original draft, Writing – review & editing. **Xiaohan Yin:** Methodology, Validation. **Fangyi Chen:** Validation, Visualization, Writing – review & editing. **Ke-Jian Wang:** Conceptualization, Supervision, Validation, Funding acquisition, Writing – review & editing.

Declaration of competing interest

The authors declare that they have no known competing financial interests or personal relationships that could have appeared to influence the work reported in this paper.

Data availability

Data will be made available on request.

Acknowledgements

This work was supported by grants provided by the Marine Biotechnology Economic Integration Service Platform from the Fujian Association for Science and Technology, Xiamen Ocean Development Bureau (grant number: 22CZP002HJ08), and the Pingtan Research Institute of Xiamen University (grant number Z20220743). We express gratitude to Dr. Bo Jun and Dr. Mohammad Arif for their constructive comments and Engineer Zhiyong Lin for technical assistance with the use of the experimental instruments.

Supplementary materials

Supplementary material associated with this article can be found, in the online version, at doi:10.1016/j.aquatox.2024.107016.

References

Abdel-Shafy, H.I., Mansour, M.S.M., 2016. A review on polycyclic aromatic hydrocarbons: source, environmental impact, effect on human health and remediation. Egypt. J. Pet. 25, 107–123. https://doi.org/10.1016/j.ejpe.2015.03.011.

Ahad, J.M.E., Jautzy, J.J., Cumming, B.F., Das, B., Laird, K.R., Sanei, H., 2015. Sources of polycyclic aromatic hydrocarbons (PAHs) to northwestern Saskatchewan lakes east of the Athabasca oil sands. Org. Geochem. 80, 35–45. https://doi.org/10.1016/j.orggeochem.2015.01.001.

Albornoz-Abud, N.A., Canul-Marín, G.F., Chan-Cuá, I., Hernández-Núñez, E., Cañizares-Martínez, M.A., Valdés-Lozano, D., Rodríguez-Canul, R., Albores-Medina, A., Colli-Dula, R.C., 2021. Gene expression analysis on growth, development and toxicity pathways of male Nile tilapia (*Oreochromis niloticus*), after acute and sub-chronic benzo (α) pyrene exposures. Comp. Biochem. Physiol. C Toxicol. Pharmacol. 250, 109160 https://doi.org/10.1016/j.cbpc.2021.109160.

Altenburger, R., Scholze, M., Busch, W., Escher, B.I., Jakobs, G., Krauss, M., Krüger, J., Neale, P.A., Ait-Aissa, S., Almeida, A.C., Seiler, T.B., Brion, F., Hilscherová, K., Hollert, H., Novák, J., Schlichting, R., Serra, H., Shao, Y., Tindall, A., Tolefsen, K.E., Umbuzeiro, G., Williams, T.D., Kortenkamp, A., 2018. Mixture effects in samples of multiple contaminants – An inter-laboratory study with manifold bioassays. Environ. Int. 114, 95–106. https://doi.org/10.1016/j.envint.2018.02.013.

Bo, J., Cai, L., Xu, J.H., Wang, K.J., Au, D.W.T., 2011. The marine medaka *Oryzias melastigma* - A potential marine fish model for innate immune study. Mar. Pollut. Bull. 63, 267–276. https://doi.org/10.1016/j.marpolbul.2011.05.014.

Bo, J., Gopalakrishnan, S., Chen, F.Y., Wang, K.J., 2014. Benzo[a]pyrene modulates the biotransformation, dna damage and cortisol level of red sea bream challenged with lipopolysaccharide. Mar. Pollut. Bull. 85, 463–470. https://doi.org/10.1016/j.marpolbul.2014.05.023.

Cao, F., Wu, P., Huang, L., Li, H., Qian, L., Pang, S., Qiu, L., 2018. Short-term developmental effects and potential mechanisms of azoxystrobin in larval and adult zebrafish (*Danio rerio*). Aquat. Toxicol. 198, 129–140. https://doi.org/10.1016/j.aquatox.2018.02.023.

Chikae, M., Hatano, Y., Ikeda, R., Morita, Y., Hasan, Q., Tamiya, E., 2004. Effects of bis (2-ethylhexyl) phthalate and benzo[a]pyrene on the embryos of Japanese medaka (*Oryzias latipes*). Environ. Toxicol. Pharmacol. 16, 141–145. https://doi.org/10.1016/j.etap.2003.11.007.

Cong, Y., Jin, F., Wang, J., Mu, J., 2017. The embryotoxicity of ZnO nanoparticles to marine medaka, *Oryzias melastigma*. Aquat. Toxicol. 185, 11–18. https://doi.org/10.1016/j.aquatox.2017.01.006.

Corrales, J., Fang, X., Thornton, C., Mei, W., Barbazuk, W.B., Duke, M., Scheffler, B.E., Willett, K.L., 2014. Effects on specific promoter DNA methylation in zebrafish embryos and larvae following benzo[a]pyrene exposure. Comp. Biochem. Physiol. C Toxicol. Pharmacol. 37–46. https://doi.org/10.1016/j.cbpc.2014.02.005.

Deng, C., Dang, F., Gao, J., Zhao, H., Qi, S., Gao, M., 2018. Acute benzo[a]pyrene treatment causes different antioxidant response and DNA damage in liver, lung, brain, stomach and kidney. Heliyon 4, e00898. https://doi.org/10.1016/j.heliyon.2018.e00898.

Deng, J., Yu, L., Liu, C., Yu, K., Shi, X., Yeung, L.W.Y., Lam, P.K.S., Wu, R.S.S., Zhou, B., 2009. Hexabromocyclododecane-induced developmental toxicity and apoptosis in zebrafish embryos. Aquat. Toxicol. 93, 29–36. https://doi.org/10.1016/j.aquatox.2009.03.001.

Dhar, K., Subashchandrabose, S.R., Venkateswarlu, K., Krishnan, K., Megharaj, M., 2020. Anaerobic microbial degradation of polycyclic aromatic hydrocarbons: a comprehensive review. Rev. Environ. Contam. Toxicol. 251, 25–108. https://doi.org/10.1007/398_2019_29.

Dong, S., Kang, M., Wu, X., Ye, T., 2014. Development of a promising fish model (*Oryzias melastigma*) for assessing multiple responses to stresses in the marine environment. Biomed. Res. Int. https://doi.org/10.1155/2014/563131, 2014.

Du, C., Fang, M., Li, Y., Li, L., Wang, X., 2000. *Smac*, a mitochondrial protein that promotes cytochrome c-dependent caspase activation by eliminating IAP inhibition. Cell 102, 33–42. https://doi.org/10.1016/S0092-8674(00)00008-8.

Elfawy, H.A., Anupriya, S., Mohanty, S., Patel, P., Ghosal, S., Panda, P.K., Das, B., Verma, S.K., Patnaik, S., 2021. Molecular toxicity of benzo(a)pyrene mediated by elicited oxidative stress infer skeletal deformities and apoptosis in embryonic zebrafish. Sci. Total Environ. 789 https://doi.org/10.1016/j.scitotenv.2021.147989.

Fang, X., Thornton, C., Scheffler, B.E., Willett, K.L., 2013. Benzo[a]pyrene decreases global and gene specific DNA methylation during zebrafish development. Environ. Toxicol. Pharmacol. 36, 40–50. https://doi.org/10.1016/j.etap.2013.02.014.

Gerbersdorf, S.U., Cimatoribus, C., Class, H., Engesser, K.H., Helbich, S., Hollert, H., Lange, C., Kranert, M., Metzger, J., Nowak, W., Seiler, T.B., Steger, K., Steinmetz, H., Wieprecht, S., 2015. Anthropogenic trace compounds (ATCs) in aquatic habitats — Research needs on sources, fate, detection and toxicity to ensure timely elimination strategies and risk management. Environ. Int. 79, 85–105. https://doi.org/10.1016/j.envint.2015.03.011.

Ghiselli, A., Serafini, M., Natella, F., Scaccini, C., 2000. Total antioxidant capacity as a tool to assess redox status: critical view and experimental data. Free Radic. Biol. Med. 29, 1106–1114. https://doi.org/10.1016/S0891-5849(00)00394-4.

Guo, B., Feng, D., Xu, Z., Qi, P., Yan, X., 2021. Acute benzo[a]pyrene exposure induced oxidative stress, neurotoxicity and epigenetic change in blood clam *Tegillarca granosa*. Sci. Rep. 2021 11 (1), 1–13. https://doi.org/10.1038/s41598-021-98354-5, 11.

He, L., He, T., Farrar, S., Ji, L., Liu, T., Ma, X., 2017. Antioxidants maintain cellular redox homeostasis by elimination of reactive oxygen species. Cell Physiol. Biochem. 44, 532–553. https://doi.org/10.1159/000485089.

He, C., Wang, C., Zhou, Y., Li, J., Zuo, Z., 2012. Embryonic exposure to benzo(a)pyrene influences neural development and function in rockfish (*Sebastiscus marmoratus*). Neurotoxicology 33, 758–762. https://doi.org/10.1016/j.neuro.2012.01.002.

Honda, M., Suzuki, N., 2020. Toxicities of polycyclic aromatic hydrocarbons for aquatic animals. Int. J. Environ. Res. Public Health 17. https://doi.org/10.3390/ijerph17041363.

Hornung, M.W., Cook, P.M., Fitzsimmons, P.N., Kuehl, D.W., Nichols, J.W., 2007. Tissue distribution and metabolism of benzo[a]pyrene in embryonic and larval medaka (*Oryzias latipes*). Toxicol. Sci. 100, 393–405. https://doi.org/10.1093/toxsci/kfm231.

Hose, J.E., Hannaht, J.B., Puffer, H.W., Landolttt, M.L., 1984. Histologic and skeletal abnormalities in benzo(a)pyrene-treated rainbow trout alevins. Arch. Environ. Contam. Toxicol. 13, 675–684.

Huang, L., Wang, C., Zhang, Y., Li, J., Zhong, Y., Zhou, Y., Chen, Y., Zuo, Z., 2012. Benzo [a]pyrene exposure influences the cardiac development and the expression of cardiovascular relative genes in zebrafish (*Danio rerio*) embryos. Chemosphere 87, 369–375. https://doi.org/10.1016/j.chemosphere.2011.12.026.

Huang, L., Zuo, Z., Zhang, Y., Wang, C., 2015. Toxicities of polycyclic aromatic hydrocarbons for aquatic animals. Int. J. Environ. Res. Public Health 17. https://doi.org/10.3390/ijerph17041363.

Huang, L., Wang, C., Zhang, Y., Wu, M., Zuo, Z., 2013. Phenanthrene causes ocular developmental toxicity in zebrafish embryos and the possible mechanisms involved. J. Hazard. Mater. 261, 172–180. https://doi.org/10.1016/j.jhazmat.2013.07.030.

Incardona, J.P., Linbo, T.L., Scholz, N.L., 2011. Cardiac toxicity of 5-ring polycyclic aromatic hydrocarbons is differentially dependent on the aryl hydrocarbon receptor 2 isoform during zebrafish development. Toxicol. Appl. Pharmacol. 257, 242–249. https://doi.org/10.1016/j.taap.2011.09.010.

Incardona, J.P., Scholz, N.L., 2017. Environmental Pollution and the Fish Heart. Fish Physiol. 36, 373–433. https://doi.org/10.1016/bs.fp.2017.09.006.

Jesus, F., Pereira, J.L., Campos, I., Santos, M., Ré, A., Keizer, J., Nogueira, A., Gonçalves, F.J.M., Abrantes, N., Serpa, D., 2022. A review on polycyclic aromatic hydrocarbons distribution in freshwater ecosystems and their toxicity to benthic fauna. Sci. Total Environ. 820, 153282 https://doi.org/10.1016/j.scitotenv.2022.153282.

Jin, Y., Zheng, S., Pu, Y., Shu, L., Sun, L., Liu, W., Fu, Z., 2011. Cypermethrin has the potential to induce hepatic oxidative stress, DNA damage and apoptosis in adult zebrafish (*Danio rerio*). Chemosphere 82, 398–404. https://doi.org/10.1016/j.chemosphere.2010.09.072.

Kang, C.K., Tsai, S.C., Lee, T.H., Hwang, P.P., 2008. Differential expression of branchial Na+/K+-ATPase of two medaka species, *Oryzias latipes* and *Oryzias dancena*, with different salinity tolerances acclimated to fresh water, brackish water and seawater. Comp. Biochem. Physiol. Part A Mol. Integr. Physiol. 151, 566–575. https://doi.org/10.1016/j.cbpa.2008.07.020.

Kim, B.M., Rhee, J.S., Jeong, C.B., Lee, S.J., Lee, Y.S., Choi, I.Y., Lee, J.S., 2014. Effects of benzo[a]pyrene on whole cytochrome P450-involved molecular responses in the marine medaka *Oryzias melastigma*. Aquat. Toxicol. 152, 232–243. https://doi.org/10.1016/j.aquatox.2014.04.008.

Knecht, A.L., Truong, L., Simonich, M.T., Tanguay, R.L., 2017. Developmental benzo[a] pyrene (B[a]P) exposure impacts larval behavior and impairs adult learning in zebrafish. Neurotoxicol. Teratol. 59, 27–34. https://doi.org/10.1016/j.ntt.2016.10.006.

Kong, R.Y.C., Giesy, J.P., Wu, R.S.S., Chen, E.X.H., Chiang, M.W.L., Lim, P.L., Yuen, B.B. H., Yip, B.W.P., Mok, H.O.L., Au, D.W.T., 2008. Development of a marine fish model for studying *in vivo* molecular responses in ecotoxicology. Aquat. Toxicol. 86, 131–141. https://doi.org/10.1016/j.aquatox.2007.10.011.

Lee, C., Kwon, B.O., Hong, S., Noh, J., Lee, J., Ryu, J., Kang, S.G., Khim, J.S., 2018. Sub-lethal and lethal toxicities of elevated CO2 on embryonic, juvenile, and adult stages of marine medaka *Oryzias melastigma*. Environ. Pollut. 241, 586–595. https://doi.org/10.1016/j.envpol.2018.05.091.

Li, Y., Wang, J., Yang, G., Lu, L., Zheng, Y., Zhang, Q., Zhang, X., Tian, H., Wang, W., Ru, S., 2020. Low level of polystyrene microplastics decreases early developmental toxicity of phenanthrene on marine medaka (*Oryzias melastigma*). J. Hazard. Mater. 385 https://doi.org/10.1016/j.jhazmat.2019.121586.

Lin, Y.C., Wu, C.Y., Hu, C.H., Pai, T.W., Chen, Y.R., Wang, W.Der, 2020. Integrated hypoxia signaling and oxidative stress in developmental neurotoxicity of benzo[a] pyrene in zebrafish embryos. Antioxidants (Basel) 9, 1–71. https://doi.org/10.3390/antiox9080731.

Lin, Q.S., 1999. Mitochondria and apoptosis. Acta. Biochim. Biophys Sin (Shanghai) 31, 118. https://doi.org/10.1126/science.281.5381.1309.

Lin, X.L., Wang, X.H., Zhao, Y.Y., Hong, H.S., Mu, J.L., Fang, C., 2011. Notice of Retraction: quantification of PAHs pollution in marine environment by measurements of EROD activity and Caspase-3/7 activity in marine medaka (*Oryzias melastigma*) embryos. In: 5th international conference on bioinformatics and biomedical engineering, iCBBE 2011. https://doi.org/10.1109/icbbe.2011.5781420.

Livak, K.J., Schmittgen, T.D., 2001. Analysis of relative gene expression data using real-time quantitative PCR and the 2(-delta delta c(t)) method. Methods 25, 402–408. https://doi.org/10.1006/meth.2001.1262.

Mao, X., Cai, T., Olyarchuk, J.G., Wei, L., 2005. Automated genome annotation and pathway identification using the KEGG Orthology (KO) as a controlled vocabulary. Bioinformatics 21, 3787–3793. https://doi.org/10.1093/bioinformatics/bti430.

Martínez-Reyes, I., Chandel, N.S., 2020. Mitochondrial TCA cycle metabolites control physiology and disease. Nat. Commun. 11 (1), 11. https://doi.org/10.1038/s41467-019-13668-3, 20201–11.

Mayer, F.L., Versteeg, D.J., McKee, M.J., Folmar, L.C., Graney, R.L., McCume, D.C., Rattner, B.A., 2018. Physiological And Nonspecific Biomarkers. Biomarkers 5–86. https://doi.org/10.1201/9781351070270-2.

Moosavi, B., Berry, E.A., Zhu, X.L., Yang, W.C., Yang, G.F., 2019. The assembly of succinate dehydrogenase: a key enzyme in bioenergetics. Cell. Mol. Life Sci. 76 (20), 76. https://doi.org/10.1007/S00018-019-03200-7, 20194023–4042.

Mu, J.li, Wang, X.hong, Jin, F., Wang, J.ying, Hong, H.sheng, 2012. The role of cytochrome P4501A activity inhibition in three- to five-ringed polycyclic aromatic hydrocarbons embryotoxicity of marine medaka (*Oryzias melastigma*). Mar. Pollut. Bull. 64, 1445–1451. https://doi.org/10.1016/j.marpolbul.2012.04.007.

Nam, S.E., Saravanan, M., Rhee, J.S., 2020. Benzo[a]pyrene constrains embryo development via oxidative stress induction and modulates the transcriptional responses of molecular biomarkers in the marine medaka *Oryzias javanicus*. J. Environ. Sci. Health A. 55, 1050–1058. https://doi.org/10.1080/10934529.2020.1767452.

Nolfi-Donegan, D., Braganza, A., Shiva, S., 2020. Mitochondrial electron transport chain: oxidative phosphorylation, oxidant production, and methods of measurement. Redox Biol. https://doi.org/10.1016/j.redox.2020.101674.

Palanikumar, L., Kumaraguru, A.K., Ramakritinan, C.M., Anand, M., 2012. Biochemical response of anthracene and benzo [a] pyrene in milkfish *Chanos chanos*. Ecotoxicol. Environ. Saf. 75, 187–197. https://doi.org/10.1016/J.ecoenv.2011.08.028.

Pannetier, P., Morin, B., Clérandeau, C., Lacroix, C., Cabon, J., Cachot, J., Danion, M., 2019. Comparative biomarker responses in Japanese medaka (*Oryzias latipes*) exposed to benzo[a]pyrene and challenged with betanodavirus at three different life stages. Sci. Total Environ. 652, 964–976. https://doi.org/10.1016/j.scitotenv.2018.10.256.

Pereira, L., 2014. Persistent organic chemicals of emerging environmental concern. In: Malik, A., Grohmann, E., Akhtar, R. (Eds.), Environmental deterioration and human health. Springer, Dordrecht, pp. 163–213. https://doi.org/10.1007/978-94-007-7890-0_8.

Redza-Dutordoir, M., Averill-Bates, D.A., 2016. Activation of apoptosis signaling pathways by reactive oxygen species. Biochim. Biophys. Acta - Mol. Cell Res. 1863, 2977–2992. https://doi.org/10.1016/j.bbamcr.2016.09.012.

Sheweita, S.A., Al-Shora, S., Hassan, M., 2016. Effects of benzo[a]pyrene as an environmental pollutant and two natural antioxidants on biomarkers of reproductive

dysfunction in male rats. Environ. Sci. Pollut. Res. 23, 17226–17235. https://doi.org/10.1007/S11356-016-6934-4.
Siddiqi, H.A., Ansari, F.A., Munshi, A.B., 2009. Assessment of hydrocarbons concentration in marine fauna due to Tasman spirit oil spill along the Clifton beach at Karachi coast. Environ. Monit. Assess. 148, 139–148. https://doi.org/10.1007/s10661-007-0145-x.
Singare, P.U., 2016. Carcinogenic and endocrine-disrupting PAHs in the aquatic ecosystem of India. Environ. Monit. Assess. 188 https://doi.org/10.1007/s10661-016-5597-4.
Smeitink, J., Van Den Heuvel, L., DiMauro, S., 2001. The genetics and pathology of oxidative phosphorylation. Nat. Rev. Genet. 2 (5), 342–352. https://doi.org/10.1038/35072063, 20012.
Storey, J.D., Tibshirani, R., 2003. Statistical significance for genome wide studies. Proc. Natl. Acad. Sci. U S A 100, 9440–9445. https://doi.org/10.1073/pnas.1530509100.
Su, W., Zha, S., Wang, Y., Shi, W., Xiao, G., Chai, X., Wu, H., Liu, G., 2017. Benzo[a] pyrene exposure under future ocean acidification scenarios weakens the immune responses of blood clam, *Tegillarca granosa*. Fish Shellfish Immunol 63, 465–470. https://doi.org/10.1016/j.fsi.2017.02.046.
Sun, D., Chen, Q., Zhu, B., Lan, Y., Duan, S., 2020. Long-term exposure to Benzo[a] Pyrene affects sexual differentiation and embryos toxicity in three generations of marine medaka (*Oryzias melastigma*). Int. J. Environ. Res. Public Health 17. https://doi.org/10.3390/ijerph17030970.
Trushin, N., Alam, S., El-Bayoumy, K., Krzeminski, J., Amin, S., Gullett, J., Meyers, C., Prokopczyk, B., 2012. Comparative metabolism of benzo[a]pyrene by human keratinocytes infected with high-risk human papillomavirus types 16 and 18 as episomal or integrated genomes. J. Carcinog. 11 https://doi.org/10.4103/1477-3163.92309.
Tsikas, D., 2017. Assessment of lipid peroxidation by measuring malondialdehyde (MDA) and relatives in biological samples: analytical and biological challenges. Anal. Biochem. 524, 13–30. https://doi.org/10.1016/j.ab.2016.10.021.
Valero-Navarro, A., Fernández-Sánchez, J.F., Medina-Castillo, A.L., Fernández-Ibáñez, F., Segura-Carretero, A., Ibáñez, J.M., Fernández-Gutiérrez, A., 2007. A rapid, sensitive screening test for polycyclic aromatic hydrocarbons applied to Antarctic water. Chemosphere 67, 903–910. https://doi.org/10.1016/j.chemosphere.2006.11.028.
Wan, Z., Chen, J., 2018. Human errors are behind most oil-tanker spills. Nature 560, 161–163. https://doi.org/10.1038/d41586-018-05852-0.
Wang, L., Scheffler, B.E., Willett, K.L., 2006. CYP1C1 messenger RNA expression is inducible by benzo[a]pyrene in *fundulus heteroclitus* embryos and adults. Toxicol. Sci. 93, 331. https://doi.org/10.1093/toxsci/kfl072.
Wills, L.P., Jung, D., Koehrn, K., Zhu, S., Willett, K.L., Hinton, D.E., di Giulio, R.T., 2010. Comparative chronic liver toxicity of benzo[a]pyrene in two populations of the Atlantic killifish (*Fundulus heteroclitus*) with different exposure histories. Environ. Health Perspect. 118, 1376. https://doi.org/10.1289/ehp.0901799.
Wills, L.P., Zhu, S., Willett, K.L., Di Giulio, R.T., 2009. Effect of CYP1A inhibition on the biotransformation of benzo[a]pyrene in two populations of *Fundulus heteroclitus* with different exposure histories. Aquat. Toxicol. 92, 195–201. https://doi.org/10.1016/j.aquatox.2009.01.009.
Wu, X., Huang, Q., Fang, C., Ye, T., Qiu, L., Dong, S., 2012. PFOS induced precocious hatching of *Oryzias melastigma*–from molecular level to individual level. Chemosphere 87, 703–708. https://doi.org/10.1016/J.chemosphere.2011.12.060.
Xiao, R., Zhou, H., Chen, C.M., Cheng, H., Li, H., Xie, J., Zhao, H., Han, Q., Diao, X., 2018. Transcriptional responses of *Acropora hyacinthus* embryo under the benzo(a) pyrene stress by deep sequencing. Chemosphere 206, 387–397. https://doi.org/10.1016/J.chemosphere.2018.04.149.
Yamaguchi, A., Uchida, M., Ishibashi, H., Hirano, M., Ichikawa, N., Arizono, K., Koyama, J., Tominaga, N., 2020. Potential mechanisms underlying embryonic developmental toxicity caused by benzo[a]pyrene in Japanese medaka (*Oryzias latipes*). Chemosphere 242, 125243. https://doi.org/10.1016/J.chemosphere.2019.125243.
Yin, X., Liu, Y., Zeb, R., Chen, F., Chen, H., Wang, K.J., 2020. The intergenerational toxic effects on offspring of medaka fish *Oryzias melastigma* from parental benzo[a]pyrene exposure via interference of the circadian rhythm. Environ. Pollut. 267 https://doi.org/10.1016/j.envpol.2020.115437.
Young, M.D., Wakefield, M.J., Smyth, G.K., Oshlack, A., 2010. Gene ontology analysis for RNA-seq: accounting for selection bias. Genome Biol 11. https://doi.org/10.1186/GB-2010-11-2-R14.
Zhao, Y., Wang, X., Lin, X., Zhao, S., Lin, J., 2017. Comparative developmental toxicity of eight typical organic pollutants to red sea bream (*Pagrosomus major*) embryos and larvae. Environ. Sci. Pollut. Res. Int. 24, 9067–9078. https://doi.org/10.1007/S11356-016-6282-4.
Zheng, Y., Li, Y., Yue, Z., Samreen, Li, Li, X., Wang, J., 2020. Teratogenic effects of environmentally relevant concentrations of phenanthrene on the early development of marine medaka (*Oryzias melastigma*). Chemosphere 254. https://doi.org/10.1016/j.chemosphere.2020.126900.
Zhu, L., Chen, Y., Zhou, R., 2008. Distribution of polycyclic aromatic hydrocarbons in water, sediment and soil in drinking water resource of Zhejiang Province. China. J. Hazard. Mater. 150, 308–316. https://doi.org/10.1016/j.jhazmat.2007.04.102.